A NEW MODEL FOR THE STEADY STATE DEFORMATION AND FRICTION OF WEBS ON ROLLERS

By

Dilwyn P. Jones
Emral Ltd.
UNITED KINGDOM

ABSTRACT

A web moving through process machinery interacts with rollers through frictional forces, which may change its direction of motion and tension. By modelling the web as a beam, these forces can be calculated from its tension, curvature and angle, at all points in contact. In turn, the forces can be combined to give distributed forward and lateral forces and a distributed moment, which determine the beam deformation. This approach was introduced in an earlier paper [1], and applied quantitatively to the "stick zone", where web and roller surface velocities match. Now it has been extended to microslip zones in steady state, the transitions to stick zones, and free spans.

A numerical model calculates the microslip zone length, variation of lateral displacement, web angle, bending moment, shear, tension and motion relative to the roller surface. In the microslip zone just before the web leaves a roller into a free span, the behaviour is surprisingly complex, with an unexpected interaction between steering and web tension, and reversal of web angle during contact. The effects of misaligned or tapered rollers, tension change, incoming web shear and camber can be examined separately and in combination.

The model has also been applied to interacting spans, where misalignment in one span steers the web in the reverse direction in the preceding span (sometimes known as "moment transfer"). Microslip occurs over the whole wrap of the roller between the two. At onset, the exit microslip zone length on this roller is equal to the wrap length: the model predicts the misalignment when this occurs. Extension to the preceding span gives agreement with the experimental results and simpler model of Good [2].

The beam equations indicate that a microslip zone at roller entry followed by a stick zone is only possible if the web shear is sufficiently large. Otherwise, there is no microslip zone, and the web strain at end of the span matches that on the roller. If the microslip zone exists, the bending moment and shear fall from their values at entry to those in the stick zone, where shear is supported by a static frictional moment.

The model provides a new, more complete picture of web behavior on rollers. It could find application in detailed analysis of steering guides, problems with cambered

webs, and the occurrence of micro-scratches from steering - alone and in combination with tension changes.

INTRODUCTION

Rollers guide the path of a web in a line, and may alter the tension by exerting friction forces. This one-dimensional textbook situation is well understood [3], and also finds application in belt drives. In steady state, the area of contact consists of a stick zone (zone of adhesion, where there is no relative motion) followed by a zone of microslip, where the tension changes gradually by a small change in web strain and speed. This picture has been extended to webs wrapping rollers driven at different speeds [4], and undergoing thermal expansion and contraction [5]. When the web is steered from its straight path by a guide, misaligned or tapered diameter roller, the forces exerted are also transmitted by friction in a microslip zone.

However, models of web lines for control dynamics and steering usually ignore the finite web length on the rollers, treating the forces as being applied at the roller exit. This may be adequate for long spans and small diameter rollers, but in wide lines the roller diameters are large and the web length on rollers may exceed that between them.

Published experiments and models have not considered the microslip zone induced by simple steering, but the treatment of each span separately with concentrated forces acting at its ends has worked well. However, the behaviour is different when the microslip zone extends over the whole contact on a roller, and steering effects are transmitted across it. The spans interact, by a process termed “moment transfer”. Studies of this give some insight into the friction forces acting during contact.

This paper describes a model for the microslip zone with steady state steering. Improved understanding and a predictive tool could help with:

- The effects of steering on wrinkling, a major cause of scrap product.
- Roller surface design through coefficient of friction.
- Scratch length prediction, important for product quality and the generation of wear debris.
- The interaction of steering and MD tension change over a roller.
- The influence of incoming web condition, such as shear strain and camber (intrinsic curvature).
- Design of web line layout, wrap and span lengths and alignment requirements.
- Design of web guides to avoid span interactions.

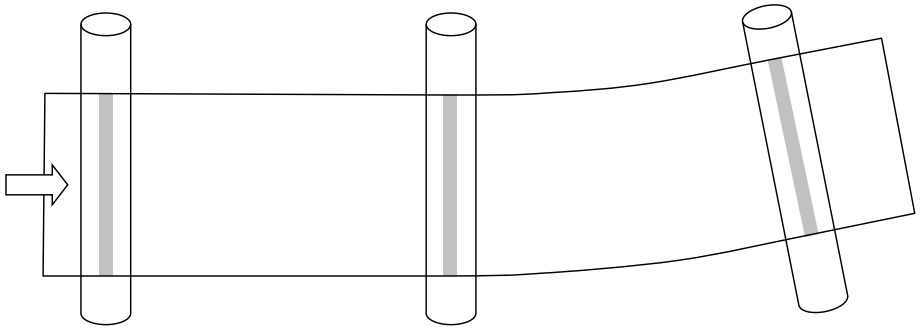

Figure 1 – Schematic View of Web Passing over Rollers Showing the Contact Patches

MODEL DEVELOPMENT

A web can be defined as a continuous flexible strip [6], and an ideal web has uniform width, thickness and properties. The tension in the machine direction (MD) as the web wraps the curved surface of a roller generates a pressure normal to the surface. If there is some contact between the web and roller surfaces, there may be a distributed friction force acting along the surface. Figure 1 shows a schematic view of the web passing over some rollers. Each contact patch may have regions where there is no relative motion between web and roller surface, termed stick zones; and regions where there is, changing the web stresses and strains, termed slip zones. If the relative movement on the roller surface is small, the term "microslip" is used instead. Friction forces are always exerted in slip and microslip zones, but may be absent in stick zones.

The web obeys the laws of continuum mechanics, and is commonly treated as a 2-dimensional membrane. Applying Newton's Second Law of Motion gives a momentum balance equation. The inertial terms are small for most web handling applications, both steady state and dynamic [7, 8]. Neglecting them results in an instantaneous mechanical equilibrium at all times. The distributed friction forces are balanced by stress gradients.

$$S_x = -h\left[\frac{\partial \sigma_x}{\partial x} + \frac{\partial \tau_{xy}}{\partial y}\right] \qquad \{1\}$$

$$S_y = -h\left[\frac{\partial \sigma_y}{\partial y} + \frac{\partial \tau_{xy}}{\partial x}\right] \qquad \{2\}$$

x and y are MD and TD coordinates. σ_x, σ_y and τ_{xy} are MD, TD and shear components of stress, S_x and S_y are the MD and TD components of the local friction force per unit area S, and h the web thickness.

The value of S is zero in the spans between rollers, and given by equation 3 during contact:

$$S \le \left(\frac{\mu T}{wR}\right) \qquad \{3\}$$

where μ is an appropriate coefficient of friction, T tension, w width and R roller radius. S may be discontinuous at the boundaries where the web enters and leaves rollers, and between stick and microslip zones. From equations 1 and 2, the stress gradients are discontinuous at the same locations. However, S is always finite so the stresses σ_x, σ_y and τ_{xy} themselves are continuous at all points on the web.

Sievers et al.[8] defined a web conveying system as "made up of a number of web spans joined at their boundaries by rollers". Instead, this paper emphasizes the continuous nature of the web, particularly as it enters and leaves contact. Consideration of separate spans obscures the continuity of material stresses and deformation that determine the system behaviour. Seeking "boundary conditions" at the ends of each span has led to some confusion, errors in modelling and unsupported assertions. Although the recent dynamic models for lateral web behaviour assuming full stick on rollers appear to be correct [9, 10], the continuous web approach gives a clearer picture of the situation, and suggests how slip can be incorporated.

Extended Timoshenko Beam Model

Shelton [7] showed that the shape of the web between rollers matches the prediction of the Euler-Bernoulli beam model, in which axial tension acts to straighten the beam. More recently, a demonstration by Brown [11], using large deformations of a low-modulus web, confirmed the behaviour qualitatively. Shelton then added shear deformation using the Timoshenko model [12], although its effect were insignificant in his tests. Sievers et al. [8] used this model, and showed that shear strain was carried from one span into the next, explaining the reappearance of lateral error downstream of a web guide, termed "weave regeneration". This has been reworked by Brown [10], using the correct boundary conditions. These models are valid only for a linearly elastic web that is uniform and flat, i.e. there are no slack areas, troughs or wrinkles.

Any beam model imposes a shape and strain distribution on the web. In the work referred to earlier, the average MD tension was taken to be constant in spans. When MD forces are present, for example from friction, the tension may vary in the MD. A simple example is the exponential rise or fall in tension, given by the belt equation [3], when there are no lateral steering effects. The model developed here extends the Timoshenko beam to include an MD variation of average tension.

The web material moves through the beam shape, and its velocity at any point is linearly related to the MD strain. In a slip zone, the local friction force opposes the direction of web motion relative to the roller surface. The force magnitude is given by equation {3} using the local value of *T/w*, also dependent on the MD strain. The calculation is described in [1].

Shelton [13] recognized that the web shape in contact determines the friction force distribution, and integrating across the width gives the net TD frictional force f_y and couple m acting at a particular MD position. The author extended this [1] to include the MD friction force, and follow the variation with MD position.

The net frictional force and couple act at each location to change the shape of the web, considered as a beam. The textbook example of a beam on an elastic foundation [14] is a simpler example where the beam shape is partly determined by forces whose magnitude depends on the shape.

Beam Equations

The equations for this Extended Timoshenko Beam are derived in [1], and shown below, simplified for small angles and strains.

$$f_x = -\frac{dT}{dx} + \kappa F \qquad \{4\}$$

$$f_y = -\frac{dF}{dx} - \kappa T \qquad \{5\}$$

$$m = -\frac{dM}{dx} + F \qquad \{6\}$$

F is the shear force, related to shear strain γ:

$$F = AG\gamma \qquad \{7\}$$

A is the section area hw and G the shear modulus incorporating the shear coefficient.

As normal for a Timoshenko beam, the total curvature comprises bending and shear contributions κ_b and κ_s. The bending curvature κ_b is taken as the sum of any intrinsic curvature (camber) κ_0 and that created by a tension gradient in *y* or bending moment *M*:

$$\kappa = \frac{d\theta}{dx} = \kappa_b + \kappa_s \quad \{8\}$$

$$\kappa_b = \kappa_0 - \frac{M}{EI} \quad \{9\}$$

$$\kappa_s = \frac{d\gamma}{dx} \quad \{10\}$$

E is Young's modulus and *I* the second moment of area, $w^3h/12$.

The local web velocity is given by $V(1 + \epsilon - \kappa_b y)$, where *V* is the speed of the roller surface and ϵ is the increase in web strain at y=0 from the value when the web and roller speeds match. For small strains and web angle, the direction of web movement relative to the roller surface ϕ is given by:

$$\sin\phi = \frac{\theta}{r} \quad \{11\}$$

$$\cos\phi = \frac{\epsilon - \kappa_b y}{r} \quad \{12\}$$

$$r = \sqrt{(\epsilon - \kappa_b y)^2 + \theta^2} \quad \{13\}$$

The MD movement changes direction at:

$$y_0 = \epsilon/\kappa_b \quad \{14\}$$

This point can be considered an "instant center" for the rotation. It may lie inside or outside the web width.

The components of friction force and friction couple are given by:

$$f_x = -\int_{-w/2}^{w/2} \left(\frac{T}{w} + \frac{Mhy}{I}\right) \frac{\mu\cos\phi}{R}\, dy \quad \{15\}$$

$$f_y = -\int_{-w/2}^{w/2} \left(\frac{T}{w} + \frac{Mhy}{I}\right) \frac{\mu\sin\phi}{R}\, dy \quad \{16\}$$

$$m = -\int_{-w/2}^{w/2} \left(\frac{T}{w} + \frac{Mhy}{I}\right) \frac{\mu y\cos\phi}{R}\, dy \quad \{17\}$$

The integrals can be solved analytically using equations {11-13}. The system of first-order differential equations {4-10} must be solved numerically when friction is acting. For a free span, however, they can be combined to give a single 3rd order differential equation for θ, or the normal 4th order equation for beam deflection, and

solved to give the familiar solution with hyperbolic functions [14]. It has been verified that the numerical solution agrees with the analytic solution of the Timoshenko beam.

The Stick Zone

The web velocity matches that of the roller surface throughout the stick zone. This leads to the requirement that the extra strain ϵ, bending curvature κ_b and web angle θ must all be zero. However, there can be a non-zero shear strain, constant in the MD. This generates a shear force, which is balanced by the frictional couple according to equation {6}. The absence of relative motion implies that static friction provides the couple. Analysis shows that a range of shear force magnitudes is possible, from zero to a maximum of F_{max} in an ideal web [1], where.

$$F_{max} = m_{max} = \mu T w / 4R \qquad \{18\}$$

Boundary Matching

At the boundaries between free spans, stick and slip zones, stress components are continuous as established above. This implies that the extra strain ϵ, bending curvature κ_b and shear strain γ are also continuous. The last two lead to the conclusion that the web angle θ and lateral displacement are also continuous. However, the gradient of shear strain may have a discontinuity, in which case the overall curvature κ may have one also.

When the web enters a stick zone immediately after a free span, this matching places requirements on the variables at the end of the span. For an ideal web without camber contacting a cylindrical roller, these can be restated as the normal entry rule ($\theta = 0$), zero bending moment and tension in the span equal to that on the roller. These are the familiar boundary conditions when the free span is considered separately.

A sequence of rollers may be misaligned and running at different speeds. The local *x-y* coordinate system and the tension at which $\epsilon = 0$ will change along the sequence: suitable rotations of axes and changes to the baseline of ϵ must be applied at the start or end of each free span.

Stick to Microslip Transition

When the web moves from the stick to microslip zone, motion relative to the roller surface starts. For the familiar case of slip in the MD only, the web tension increases or decreases, linearly with position at first. In equation {4}, the friction force jumps from zero, giving a discontinuity in tension gradient. The tension change continues through the microslip zone, following the exponential Belt Equation, until the tension in the free span is reached at the end.

When steering effects are also present, a combination of rotation and MD slip is possible, leading to linear changes in bending moment and possibly tension. Analysis in [1] suggested that a linear increase in shear force cannot occur in addition. The second possibility of a linear increase in shear force alone has not yet been encountered in the simulations.

Microslip to Stick Transition

Friction always opposes the direction of relative movement, so equations {4-6} tends to give a gradient of tension, shear force or bending moment that takes the variable further from the value in the stick zone as *x* increases. As a result, there appears to be no steady state microslip zone preceding the stick zone (i.e. at roller entry) in most cases.

However, it is clear that large misalignment could produce a shear force on entry that exceeds the value that can be supported by static friction (equation {18}). It seems reasonable to expect the shear force in the stick zone to be at that limit, and fall to that value in the microslip zone, accompanied by a drop in bending moment to zero. Analysis to show how this happens has not yet been successful.

All cases examined in the rest of this paper will assume that a stick zone extends back to the entry of the steering roller, implying a high coefficient of friction. The boundary conditions at entry are therefore matching of average speed ($\epsilon = 0$), zero bending curvature and web angle. Web displacement and shear force are unknown.

Exit Microslip Zone

Just before the exit of a roller, the web variables change continuously from their values in the previous stick zone to those at the start of the free span. As the coefficient of friction increases, the zone becomes shorter. In the limit of zero zone length, the lateral displacement and face angle are continuous across the zone. However, the bending moment, tension, web angle and shear force have a step in value, with the last 2 linked to maintain constant face angle.

When the web span is analyzed on its own, the lateral position and face angle at entry are boundary conditions, but the bending moment, tension and the web angle are unknown. Returning to a finite length microslip zone, there must also be 3 unknowns. One is the zone length, and the others relate to how the slip movement starts: the instant center location and presumably how the web angle starts to change. This cannot be linear as noted as above, but probably has an unknown quadratic or higher order coefficient.

Numerical Solution of Equations

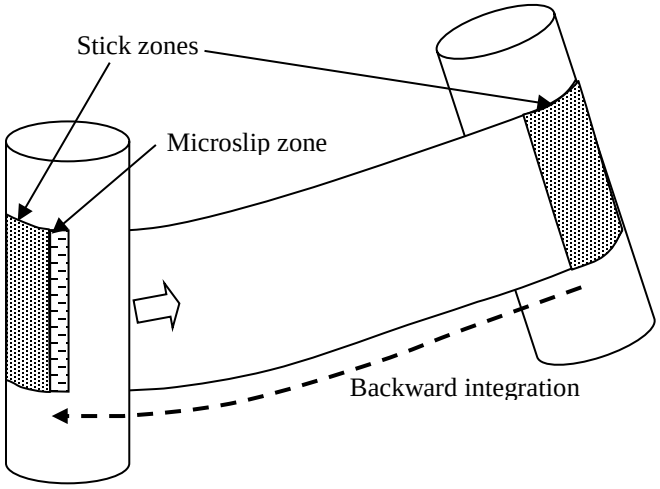

Figure 2 – Exit Microslip Zone and Free Span, Showing Backward Integration Direction

As noted in [1], the set of first order equations can be solved either forwards or backwards in the region between the stick zone boundaries. The difficulties arise because of the unknown microslip zone length and the boundary conditions specified at both ends of the region. It is easier to integrate the equations in the backward direction, and use a binomial search method to find the value of shear force at the downstream roller that

satisfies the boundary conditions at the start of the exit microslip zone (figure 2). VBA for Microsoft Excel® was used.

Equations {5-6} were rearranged in terms of *F* and *M*, then discretized using a constant negative step length. At the mid-point of each interval, $F = (F_{i+1} + F_i)/2$ and $dF/dx = (F_{i+1} - F_i)/\Delta x$, similarly for *M*. The resulting simultaneous equations were solved for F_{i+1} and M_{i+1}, using the tension and friction forces evaluated at step *i*. Finally, the tension and forces were evaluated for step *i*+1.

The first part of the solution is for the free span, where the friction forces are zero. The second is for contact on the roller, and ends when the bending moment changes sign. In all cases run, the tension crosses the stick zone value within the same step. The microslip zone length was estimated by interpolating *M* within the step. The web angle approached zero more gradually, sometimes with sign changes. The shear force *F* at the zone end was compared with the boundary value in the stick zone, and an interval halving technique used to iterate towards the correct solution.

EXIT MICROSLIP ZONE EXAMPLE

Model Parameters

The experiments of Good [2] provide lateral displacement and force measurements due to misalignment, both with and without interaction between spans. The section of web line is shown in figure 3. Rollers A and B are aligned, but roller C is angled in the horizontal plane and steers the web laterally. For low angles, displacement is confined to span BC, i.e. the entry span for roller C. As the angle is increased, the web starts to deflect in the opposite direction in span A, due to interaction between the spans, and microslip occurring over the whole of roller B.

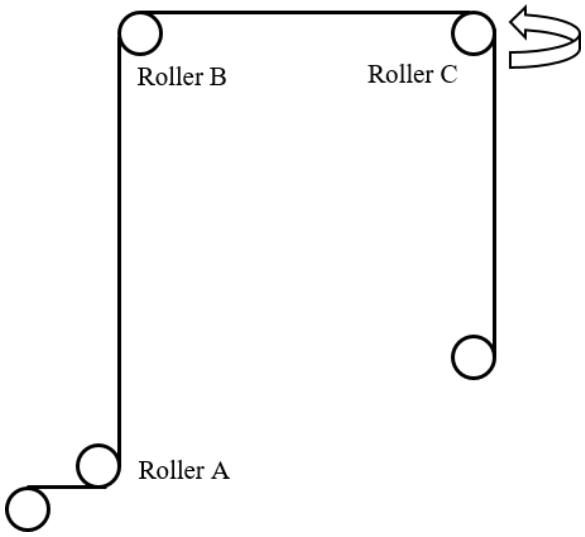

Figure 3 – Geometry for Simulations from [2]

Table 1 gives process parameters for an experimental point taken from figure 13 in [2] where misalignment is sufficient for the spans to interact.

Roller Radius	36.85 mm
Span AB length	813 mm
Span BC length	610 mm
Roller C angle	0.012 rad
Web width	152.4 mm
Web thickness	35.6 μm
Young's Modulus	3.8 GPa
Shear Modulus (estimate, with beam shear factor)	1.5 GPa
Friction Coefficient (below 50 m/min)	0.26
Web tension	66.7 N

Table 1 – Parameters to Model Web Steering in Figure 3

The new model was used to simulate roller B and span BC, assuming a stick zone at the entry to roller C and stick followed by microslip on roller B. The web was assumed to have zero intrinsic curvature and shear strain as it enters roller B. The interaction between spans BC and AB was prevented by increasing the wrap angle on roller B so it exceeded the exit microslip zone length. The length of the microslip zone was calculated as 84 mm. This is larger than the actual wrap on roller B (58 mm), confirming that interacting spans should be expected in Good's experiment.

Comparison with and without Exit Slip Zone

Table 2 compares results from the new model with the Timoshenko beam model for the span alone. The microslip zone allows the bending moment and shear force to be lower at roller B exit, increasing the web angle when it leaves the roller. Presumably this lowers the overall strain energy. As a result, the web moves laterally slightly on the roller, and an increased amount in the span because of the web angle at the start. Intuitively, this behaviour might be expected: the exit microslip zone increases the effective span length, leading to increased displacement and lower forces.

	This model	Timoshenko
Displacements (mm)		
Roller B exit	0.02	0
Roller C entry	5.31	5.01
Span BC	5.29	5.01
At Roller B Exit:		
Web angle (mrad)	1.8	0.4
Bending moment (N m)	-1.41	-1.60
Shear Force (N)	2.77	3.14

Table 2 – Model Results for Exit Slip Zone and Span, Compared with Span Alone

Bending Moment and Tension

However, looking at the behaviour in the microslip zone leads to some unexpected results. Figure 4 shows the variation of bending moment on roller B. It rises in a more or less linear fashion to a sharp maximum at the exit. Figure 5 shows the variation of tension. It follows an approximate parabolic curve, with a minimum 10% below the value in the stick zone and at the roller exit. Figure 6 shows the calculated instant center position, calculated with equation {14}. It starts close to one web edge, then moves to

the web center at the exit point. If the misalignment is reversed, the bending moment and instant center location become positive but the tension curve remains the same.

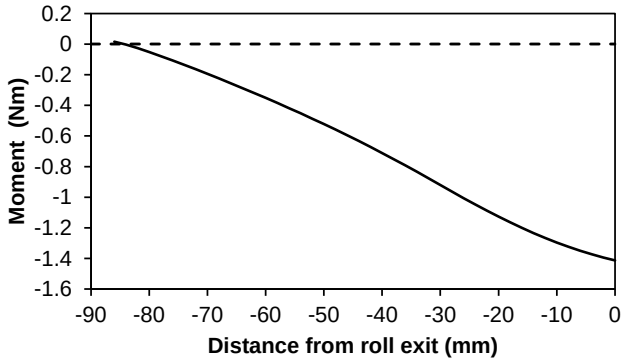

Figure 4 – Variation of Bending Moment in the Exit Slip Zone

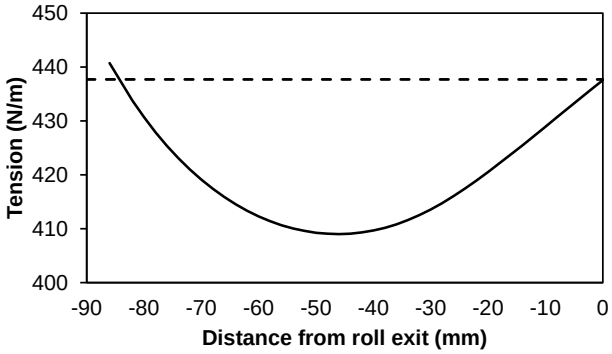

Figure 5 – Variation of Tension in the Exit Slip Zone

There is clearly an interaction between the bending moment and tension. At the roller exit, the tension is the value in the span, fixed at entry to the next roller C. In this example, it is also the value which matches speed on the roller B: as a result, the instant center is at the web center. The bending moment at the roller exit produces a larger tension change on the tight side than on the slacker side, therefore the average tension just before exit must be lower, and the instant center is closer to the tight edge.

Further back in the contact, the bending moment is still increasing away from zero at the start of the zone. The average web speed is now somewhat lower than the roller speed, and that sets up a falling average tension, again starting at the value in the stick zone.

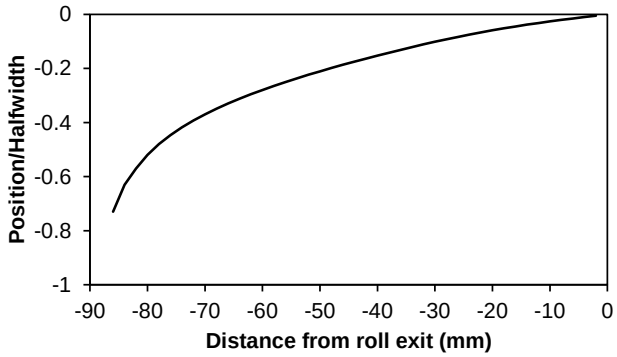

Figure 6 – Variation of Instant Center Position in the Exit Slip Zone

Shear and Lateral Effects

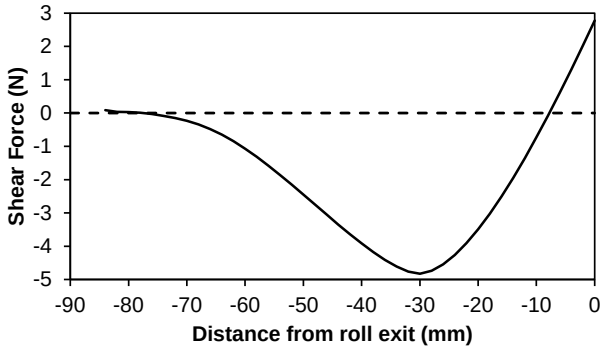

Figure 7 – Variation of Shear Force in the Exit Slip Zone

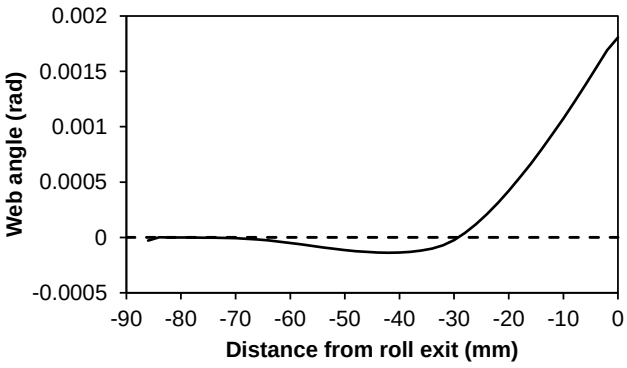

Figure 8 – Variation of Web Angle in the Exit Slip Zone, with Downstream Steering Angle 0.012 Rad

The variation of shear force, shown in figure 7, is even more surprising. It falls to -5 N in the microslip zone before rising to the exit value of 3 N. This is linked to the web angle on the roller, shown in figure 8. This starts off by falling to a small negative value before crossing zero and rising up to the exit value. In a similar way, the web displacement (figure 9) starts off negative before rising to the positive exit value.

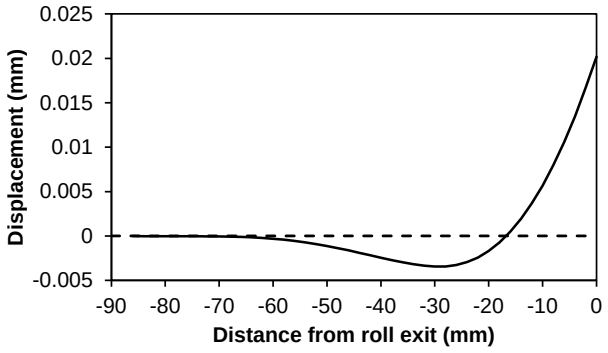

Figure 9 – Variation of Web Displacement in the Exit Slip Zone

The numerical integration scheme does not treat the angle crossing zero correctly. Somewhere in the step, f_y changes sign, but it is treated as having the constant value that it had at the start of the step. The effect of this was checked by interpolating to values at the zero crossing, taking this point as the end of a shorter step, then restarting the integration with zero f_y. The results did not change significantly. Additionally, a forward integration taking initial conditions about halfway before the zero crossing, gave very similar results through the rest of the zone and the span. Therefore, the change of angle and reversal of shear force are thought to be real effects.

Closer to the start of the microslip zone, the web angle and shear force are small and cross zero again. This is likely to be "calculation noise", and a better integration scheme may clarify the position. Also, an analytic solution may reveal the true behaviour.

Web Movement on the Roller

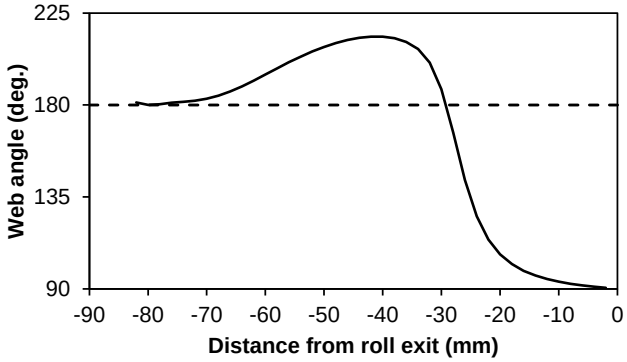

Figure 10 – Variation of Relative Movement Direction

Figure 10 shows the direction the center of the web moves relative to a point on the roller surface during the contact. Initial movement is backwards, causing the fall in tension. Then it moves towards negative *y*, turns back and finally leaves the roller in the positive *y*-direction.

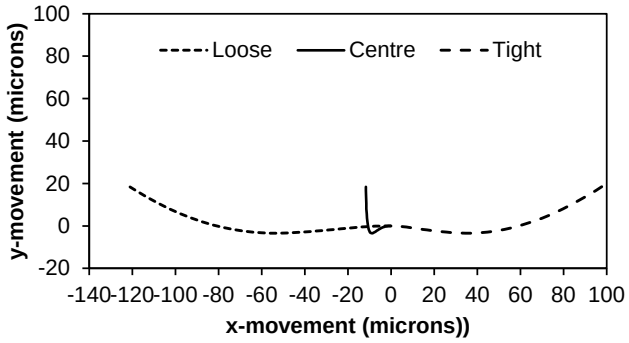

Figure 11 – Relative Movement of Points on the Web and Roller

Figure 11 traces the actual movement of points in the web center and at each edge during contact. All show the same net y-movement of 20 microns, taking place near the exit after initial movement in the opposite direction. However, the two edges are dominated by MD movement in opposite directions. This reflects the increase in bending moment. Asperities on the roller or particulate contamination would be expected to generate a scratch of these dimensions due to the movement in the microslip zone.

PARAMETRIC STUDY

It is very easy to run the model for different input parameters. As expected, the microslip zone is longer for greater misalignment. It equals the wrap length in the experiments of Good [2] at a misalignment of 8 mrad, which is consistent with the data but a little larger than his model prediction.

Variable	Base Case	Exit Tension		Initial shear		Intrinsic curvature	
Tension (N)	66.7	53.4	80.0	66.7	66.7	66.7	66.7
Initial shear strain ($\times 10^{-4}$)	0	0	0	-2.6	2.6	0	0
Radius (m)	0	0	0	0	0	-100	100
Zone length (mm)	84	110	74	78	91	92	79
Lateral displacement at span end (mm)	5.31	5.38	5.29	5.35	5.27	5.32	5.30
At roller exit							
Displacement (mm)	0.020	0.030	0.017	0.026	0.016	0.021	0.020
Moment (N m)	-1.41	-1.35	-1.44	-1.39	-1.43	-1.81	-1.02
Shear force (N)	2.77	2.57	2.92	2.73	2.82	2.76	2.78

Table 3 – Parametric Study Results

The effect of changes in exit tension, initial shear strain and intrinsic curvature are shown in Table 3. All other parameters are the same as in the previous example.

Exit Tension

The tension at which the web and roller speeds match is unchanged at 66.7 N. Columns 3 and 4 show the effect of a 10% decrease or increase in tension set at the next roller. The tension changes in the microslip zone, and remains virtually constant in the span. In the absence of steering, the zone length can be calculated as 36 and 26 mm for tension decrease and increase respectively.

When steering of 0.012 rad is included, the zone length decreases as tension increases, and vice versa. This is a little surprising: the tension increase might be expected to require additional microslip. This can be explained by the increased tension also increasing friction force, and this shortens the microslip zone which is mostly caused by steering. For steering below 0.007 rad, the zone is longer for the higher tension, because the microslip is now mostly caused by the tension change.

The trends of lateral displacement, bending moment and shear force at the roller exit reflect the changes in zone length caused by tension. The changes caused by 10% tension decrease are larger than for the same size increase.

Initial Shear

For these runs, the web in the stick zone is given a shear strain of $\pm 2.6 \times 10^{-4}$. This is the magnitude of the shear strain at the end of the span for the base case, to choose a typical value. It is considerably less than the maximum that can be supported in the stick zone, 0.0022.

The negative initial shear, which would result from steering in the opposite direction in the previous span, increases the lateral displacement at the end of the span and decreases the microslip zone length, bending moment and shear force at the roller exit. The shear strain on the next roller is only slightly reduced by 4×10^{-6}. Positive initial shear has the opposite effects.

Intrinsic Curvature

A web with camber or intrinsic curvature has a bending moment even when running straight. This may introduce some bias in the model results to one side or the other. A severe camber (small radius) of 100 m was chosen, although this is still well below the value to give edge slackness under the tension in the example.

When the camber direction opposes the steering, the microslip zone length is longer and the shear force slightly lower. Surprisingly, there is a larger displacement at the end of the span. The change in bending moment at the roller exit is due to adding 0.4 Nm, the value in the straightened curved web. The effects reverse when the camber and steering are in the same direction.

Steering Tendency of a Cambered Web

The above results show slight additional steering to the tight side of the cambered web. Other possible reasons for steering with camber web were explored with the model.

With parallel rollers and no tension change. the model produced the solution proposed by Shelton [15] that the web can run straight; i.e. zero curvature and a constant bending moment. There are no shear strains.

If the web can reduce its strain energy by developing part of the intrinsic curvature, this is likely to require some movement in a microslip zone and result in a shear strain and shear force at the end of the next span. The model was used to search (by hand) for

solutions with non-zero values of downstream shear force: none were found. Therefore it appears that cambered web does not steer in a web line which is perfectly aligned with constant tension.

However, when the web is slipping on the roller, the tension gradient towards the tighter side produces a friction force gradient in the same direction, and hence a frictional couple. Therefore, a simple tension change could cause lateral movement of a cambered web, whereas a straight web would develop an MD friction force uniform across the width, and not steer laterally. Table 4 show some results from model runs on a cambered web changing tension in the exit microslip zone. The steering directions are reversed if the camber direction is reversed.

Tension change	-10%	+10%
Microslip zone length (mm)	36	28
Span lateral displacement (mm)	-0.0019	+0.0040
Maximum or minimum		
Bending moment (N m)	0.472	0.348
Shear force (N)	0.140	-0.167
At roller exit		
Bending moment (N m)	0.398	0.402
Shear force (N)	0.0025	-0.0057

Table 4 – Model Results for Tension Change in a Cambered Web

There is a small steering effect, to the long side when tension falls, and to the short side when it rises. The microslip zone lengths are virtually unchanged from the value to create the tension change for a straight web. The tension falls or rises smoothly through the zone. However, the bending moment magnitude has a maximum in the zone for a tension fall, and a minimum for a tension rise, before coming back close to the value for a straight web at the roller exit. The shear force behaves similarly. The initial web CD movement is opposite to the final steering direction.

This steering is small, but will increase with tension change (and lower entry tension, longer spans, lower friction coefficient). Now there is a theory to compare with measurements. The model shows how the steering direction changes depending on whether the roller is driving (tension fall) or braking (tension rise). This may partly account for the lack of consensus on the direction a cambered web will steer.

INTERACTING SPANS

As a final illustration of the model, the behaviour of the base case was modelled when there is full slip on roller B in figure 3, i.e. there is insufficient wrap angle to accommodate the length of microslip zone needed after a stick zone. Roller A was modelled with high friction, so the bending moment and tension are not prescribed at this point, but the face angle is zero.

Figure 12 shows the variation of lateral displacement through the 2 spans and on the roller. The behaviour observed experimentally is observed. Table 5 compares the predictions with the results shown in figures 12 and 13 of Good [2].

The agreement is not perfect. The model displacements are larger in the direction of steering by roller C. The TD force on each roller is calculated from the shear at the contact lines and is positive in the direction of steering by roller C. The force on roller C has an unknown contribution from the exit span which is taken as zero. The model force

predictions are close to double the experimental values, but their sum is close to zero in both cases.

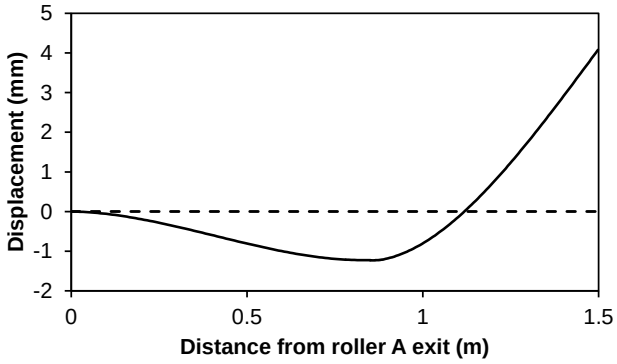

Figure 12 – Lateral Displacement in Interacting Spans.

	Model	Experiment
Displacement (mm)		
Roller B exit	-1.2	-1.7
Roller C entry	4.0	2.8
CD force on roller (N)		
Roller A	-1.1	-2.6
Roller B	3.9	6.1
Roller C	-2.1	-3.8
Total bending moment on roller B (N m)	1.01	1.04*

Table 5 – Model Results for Interacting Spans Compared with the Results of Good [2].
* - Calculated Using his Model.

In [2], Good used a simple equation for the change in bending moment across roller B, assuming the whole web is rotating about a point on its centerline. The close agreement of that calculation with the present model shows that most of the friction force acting is producing the change in bending moment, and only a small fraction is altering tension and shear force: equation 6 is dominant.

Again, the way the web variables change on the roller provides insight and some surprises. Much as predicted by early models for moment transfer [16], the bending moment (figure 13) is a maximum at Roller B exit, increasing smoothly to that value during contact, from a smaller but non-zero value at entry. In the span AB, the moment reverses direction, much as predicted for steering by a downstream moment.

Simple mechanics shows that the difference in tension between entry and exit of roller B is equal to the torque supplied to the center of the roller. In the first run of the model, the speeds of rollers B and C were set equal, but this gave a tension rise of 4 N. To achieve zero tension difference required roller B to turn more quickly, to match a tension about 10% higher than the value at roller C. The tension on the roller (figure 14) now falls to a minimum value 3% below the line tension then rises to the same value at exit.

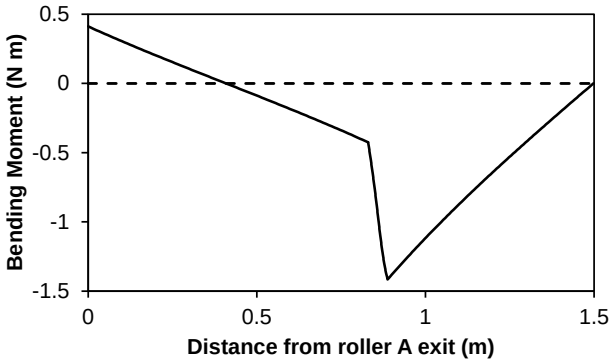

Figure 13 – Bending Moment in the Two Spans and on Roller B

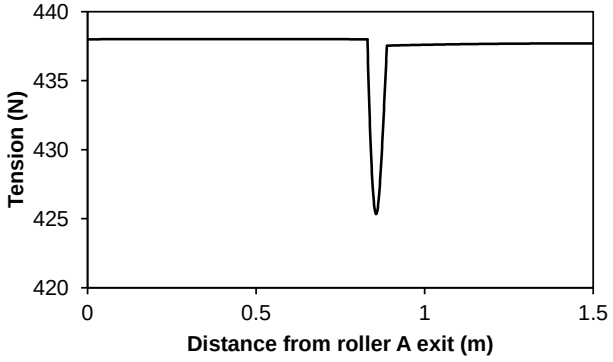

Figure 14 – Tension in the Two Spans and on Roller B Running over Line Speed

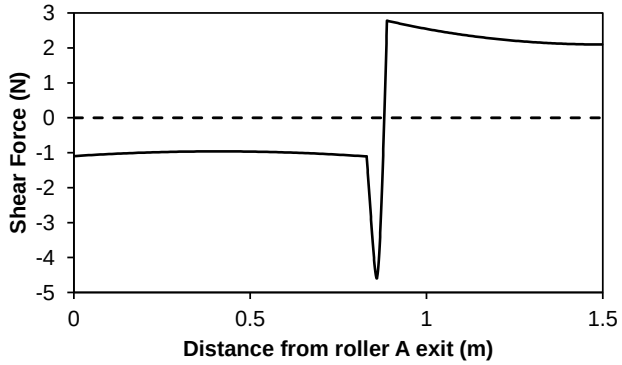

Figure 15 – Shear Force in the Two Spans and on Roller B

The shear force (figure 15) is nearly constant in each span, consistent with the gradient of bending moment. However, on roller B, the negative entry value increases by a factor of nearly 5 before falling, crossing zero and rising to the exit value.

The web angle (figure 16) is negative in span AB, but returns to a value close to zero at the contact line on roller B. It then becomes more negative again, and is constant at a low negative value for some distance. Finally it rises, gradually at first, crosses zero and reaches about a tenth of the steering angle at the exit line. The relative movement direction is close to MD at entry for much of the contact, but rotates close to the TD at the exit. In span BC, the web angle rises to the steering angle, with some curvature caused by the MD tension.

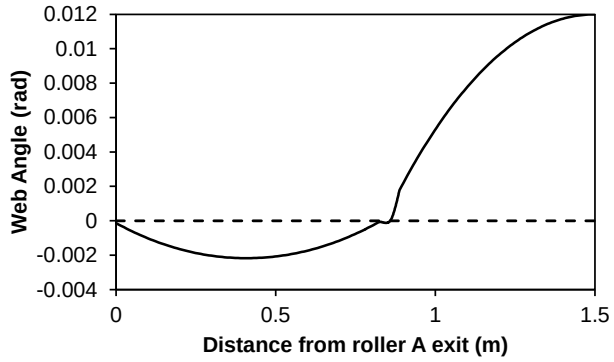

Figure 16 Web Angle in the Two Spans and on Roller B.

In this example, the "normal entry rule" is obeyed approximately but not exactly, similar to findings noted by Shelton [13].

DISCUSSION AND CONCLUSIONS

Interacting Spans

The differences between the model and Good's experimental results [2] noted above could be partly due to factors which are not modelled, such as:

- Non-zero tension change on Roller B
- Microslip zone at the exit of Roller A
- Shear strain in the incoming web affecting the steering in span AB.

However, Good's own model fits his data well. Shelton [13] assessed the agreement of his model with Good's results as good, but by eye the deviations are similar to those found here.

The model of Dobbs and Kedl [17] agrees with the results they obtained with similar tests. However, they treated the web in each span as an Euler beam, without including tension and shear effects. Their treatment of friction forces allowed the web on the roller to develop a piecewise linear variation across the width, whereas here a constant gradient is enforced by assuming the web deforms as a beam. Their model allows some interaction of the spans before full moment transfer occurs: this feature is absent in the models of Shelton, Good and the present author.

The model results reported above confirm that the above authors' assumptions are reasonable: friction gives a bending moment change on the roller close to a simple estimate from tension, and the normal entry rule is approximately obeyed.

Web Behaviour during Microslip Exit Zone

The limited number of cases run so far prevents general conclusions being drawn. However, it does appear that the exit microslip zone allows the web variables to change from the values in the stick zone to values at the roller exit. In particular, the bending moment increases smoothly. The values of bending moment and shear force at exit are lower than they would be without a microslip zone. The steering displacement downstream is slightly larger, mostly because the web angle starts to change on the roller rather than at the exit.

When there is a bending moment in the web on a roller, the local tension on the tight side changes more rapidly than on the looser side. If the instant center of the rotation is on the web centerline, the average tension increases as a result. Alternatively, maintaining a constant average tension would need the instant center to be displaced towards the tight side. This interaction of bending moment and tension causes the tension to show an unexpected dip in the microslip zone.

The web angle, displacement and shear force also show unforeseen behaviour, with the initial changes opposite to the values at the roller exit.

The model results are influenced by many parameters: roller diameter, coefficient of friction, web width, span length, web modulus, misalignment, entry and exit tensions. There are small steering effects from incoming shear strain, and camber interacting with a tension change, steering from a misaligned downstream roller, or both.

Model Performance

The web behaviour does seem to be captured by the model, but some inaccuracies may remain. There is scope to improve both the analytic treatment when the web starts to move in the exit microslip zone, and when an entry microslip zone followed by a stick zone might develop. The numerical solution method could be improved to treat zero crossings properly, locate the zone end accurately, and alternative integration techniques tried.

The problem analysis may also be applicable to turn bars inclined at 45 deg to the web direction. The small angle approximation used is clearly no longer valid, and the beam theory may need modification to take sections parallel to the roller axis rather than normal to the centerline.

In Summary

It is hoped this new model will prove useful, especially after some improvement and further exploration of parameters. The successful beam bending approach of Shelton has been employed, without additional assumptions. Calculation of the friction forces during microslip is non-trivial but has been achieved. The numerical solution has given new insight into the behaviour of webs on rollers.

REFERENCES

1. Jones, D. P., "The Behavior of a Flexible Web in Contact with a Roller," Proceedings of the Twelfth International Conference on Web Handling. Ed. Good, J. K., Oklahoma State University, 2013, to be published.
2. Good, J. K., "Shear in Multispan Web Systems," Proceedings of the Fourth International Conference on Web Handling, Ed. Good, J. K., Oklahoma State University, 1997, pp. 264-286.
3. Johnson, K. L., Contact Mechanics, Cambridge University Press, Cambridge, 1985.

4. Zahlan, N., and Jones, D. P., "Modeling Web Traction on Rollers," Proceedings of the Third International Conference on Web Handling, Ed. Good, J. K., Oklahoma State University, 1995, pp. 156-171.
5. Jones, D. P., McCann, M. J., and Abbott, S. J., "Web Tension Variations Caused by Temperature Changes and Slip on Rollers," Proceedings of the Eleventh International Conference on Web Handling, Ed. Good, J. K., Oklahoma State University, 2011.
6. Web Handling Research Center website.
7. Shelton, J. J., "Lateral Dynamics of a Moving Web," Ph.D. Thesis, Oklahoma State University, July 1968.
8. Sievers, L., Balas, M. K., and Flowtow, A., "Modeling of Web Conveyance Systems for Multivariable Control," IEEE Transactions of Automatic Control, Vol. 33, No. 6, June 1988.
9. Benson, R. C., "Lateral Dynamics of a Moving Web With Geometrical Imperfection," ASME Journal of Dynamic Systems, Measurement, and Control, Vol. 124, March 2002.
10. Brown, J. L., "The Effect of Mass Transfer on Multi-Span Lateral Dynamics of a Uniform Web," to be published in Proceedings of the Fourteenth International Conference on Web Handling, ed. Good, J. K., 2017.
11. Brown, J. L., "The Deformations and Stresses That Move Webs and the Two Rules That Govern Them," AIMCAL Applied Web Handling Conference, 2006.
12. Timoshenko, S. P., and Gere, J. M., Theory of Elastic Stability, McGraw Hill, New York, 1961.
13. Shelton, J. J., "Interaction Between Two Web Spans Because of a Misaligned Downstream Roller," Proceedings of the Eighth International Conference on Web Handling, ed. Good, J. K., 2005, pp. 101-120.
14. Young, W. C., and Budynas, R. G., Roark's Formulas for Stress and Strain, 7th ed., McGraw Hill, New York, 2002.
15. Shelton, J. J., "Effects of Web Camber on Handling," Proceedings of the 4th International Conference on Web Handling, ed. Good, J. K., 1997, pp. 248-264.
16. Young, G. E., Shelton, J. J., and Fang, B., "Interaction of Web Spans: Part I, Statics," ASME Journal of Dynamic Systems, Measurement and Control, Sep. 1989.
17. Dobbs, J. N. and Kedl, D. M., "Wrinkle Dependence on Web Roller Slip," Proceedings of the Third International Conference on Web Handling, Ed. Good, J. K., Oklahoma State University, 1995, pp. 366-381.